ELSEVIER

Journal of the Mechanics and Physics of Solids
53 (2005) 227–248

JOURNAL OF THE
MECHANICS AND
PHYSICS OF SOLIDS

www.elsevier.com/locate/jmps

Brittle fracture dynamics with arbitrary paths III. The branching instability under general loading

M. Adda-Bedia*

Laboratoire de Physique Statistique de l'Ecole Normale Supérieure, 24 rue Lhomond, F–75231 Paris Cedex 05, France

Received 14 November 2003; received in revised form 14 May 2004

Abstract

The dynamic propagation of a bifurcated crack under arbitrary loading is studied. Under plane loading configurations, it is shown that the model problem of the determination of the dynamic stress intensity factors after branching is similar to the anti-plane crack branching problem. By analogy with the exact results of the mode III case, the energy release rate immediately after branching under plane situations is expected to be maximized when the branches start to propagate quasi-statically. Therefore, the branching of a single propagating crack under mode I loading should be energetically possible when its speed exceeds a threshold value. The critical velocity for branching of the initial single crack depends only weakly on the criterion applied for selecting the paths followed by the branches. However, the principle of local symmetry imposes a branching angle which is larger than the one given by the maximum energy release rate criterion. Finally, it is shown that an increasing fracture energy with the velocity results in a decrease in the critical velocity at which branching is energetically possible.

Keywords: A. Crack branching and bifurcation; Dynamic fracture; Stress intensity factors; B. Crack mechanics; C. Analytic functions

1. Introduction

The bifurcation of the crack tip into two or more branches is a well-known phenomenon in brittle crack propagation (Ravi-Chandar and Knauss, 1984; Fineberg et al., 1992; Gross et al., 1993; Sharon et al., 1995; Sharon and Fineberg, 1996,

* Fax: +33-1-44-32-34-33.
E-mail address: adda@lps.ens.fr (M. Adda-Bedia).

0022-5096/$ - see front matter © 2004 Elsevier Ltd. All rights reserved.
doi:10.1016/j.jmps.2004.06.001

1999; Boudet et al., 1996; Boudet and Ciliberto, 2000). Recent experiments on PMMA and glass samples (Sharon et al., 1995; Sharon and Fineberg, 1996, 1999) have established that the branching phenomenon results from the dynamic instability of a single propagating crack. The instability occurs when the crack speed exceeds a critical velocity v_c, which depends neither on the applied stress nor on the geometry of the plate. Above v_c, a single crack is no longer stable. Instead, a repetitive process of micro-branching occurs, which changes the crack dynamics. Simultaneously, the acoustic emission from the crack tip region increases (Gross et al., 1993; Boudet et al., 1996; Boudet and Ciliberto, 2000), the crack velocity develops strong oscillations. In addition a pattern which is correlated with the velocity oscillations, is created on the fracture surface (Fineberg et al., 1992). Crack branching has also been observed in simulations of dynamic crack propagation using molecular dynamics (Abraham et al., 1994), finite element calculations of constitutive equations on a lattice (Xu and Needleman, 1994), numerical simulations using a phase field model of brittle fracture (Lobkovsky and Karma, 2004; Henry and Levine, 2004), and by modeling the elastic medium as a two-dimensional lattice of coupled springs (Marder and Gross, 1995).

Yoffe (1951) observed that for crack speeds less than a critical velocity v_y, the transverse tensile stress in the vicinity of a crack tip reaches its maximum along the direction of crack growth. For crack speeds larger than v_y, this component of the stress develops a maximum along two other symmetric directions. Yoffe suggested that this modification of the local singular stress field could account for the observation that rapidly growing cracks in brittle materials bifurcate into branched cracks. Since then, the origin of the branching instability has been discussed elsewhere (Freund, 1990; Adda-Bedia et al., 1996). However, all the theoretical attempts to explain the branching predict critical speeds larger than the experimental ones. A possible cause for the failure of theory is that it was focused on the stress distributions around the tip of a single straight crack, prior to branching. These analyses indicate that the stress field around the crack tip is deformed at high velocities; however, this does not provide us with a crack growth or a branching criterion.

As in the single crack case, a growth criterion for a branched crack must be based on the equality between the energy flux into the two propagating tips and the surface energy which is added as a result of this propagation (Griffith, 1920). Eshelby proposed this approach (Eshelby, 1970; Rice et al., 1994), posing the question of how large the single crack speed must be so that there will be enough energy available to form two slow cracks instead of a single fast one. Since after branching twice as much surface area is created, the branches would not advance unless their velocity is lower than that of the single crack. The simplest branched configuration that Eshelby analyzed is the idealized limiting case where the branches subtend a vanishingly small angle and both prolong the original crack plane. In this case, the energy release rate of two branches propagating at velocity v', equals twice that of a single crack moving at velocity v, and it is maximal when the branches velocity is $v' \to 0$. For the mode III case, Eshelby reported $v = 0.6c_s$, where c_s is the shear wave speed, as the minimum speed which allows branching or surface roughening (Eshelby, 1970). This result remained a rough estimate, as no full dynamic solution was available for two branches with an arbitrary angle between them.

Recently, a method for determining the elastodynamic stress fields associated with the propagation of anti-plane kinked or branched cracks has been developed (Adda-Bedia and Arias, 2003; Adda-Bedia, 2004). Particularly, the dynamic propagation of a bifurcated crack under anti-plane loading was considered (Adda-Bedia, 2004). It was shown that the corresponding model problem admits a self-similar solution, which is a convolution integral of a known kernel and a harmonic function that satisfies a simple integral equation. The dependence of the stress intensity factor immediately after branching was determined as a function of the stress intensity factor immediately before branching, the branching angle and the instantaneous velocity of the crack tip. The jump in the dynamic energy release rate due to the branching process was also computed. When applying the Eshelby's growth criterion for a branched crack, it has been shown that the minimum speed of the initial single crack which allows branching is equal to $0.39c_s$. At the branching threshold, the corresponding bifurcated cracks start their propagation at a vanishing speed with a branching angle of approximately 40° (Adda-Bedia, 2004).

The present work is an attempt to generalize the approach of (Adda-Bedia and Arias, 2003; Adda-Bedia, 2004) to the dynamic propagation of a bifurcated crack under arbitrary loading. Especially, under plane loading configurations, the dynamic stress intensity factors immediately after branching are studied. It is shown that the formulation of the corresponding model problem is identical to the anti-plane case. The difficulty for solving the branching problem under plane loading configurations completely lies in the existence of two characteristic wave speeds and in the vectorial nature of the displacement field. However, this analogy allows for the reasonable hypothesis that under plane loading configurations, the jump in the energy release rate due to branching is maximized when the branches start to propagate quasi-statically. Using Eshelby's approach, the branching of a single propagating crack under mode I loading is found to be energetically possible when its speed exceeds a threshold value. The critical branching parameters depend of the criterion applied for the selection of the paths followed by the bifurcated cracks. For instance, the maximum energy release rate criterion (Erdogan and Sih, 1963) or the principle of local symmetry (Gol'dstein and Salganik, 1974). It is found that the critical velocity for branching of the initial single crack is weakly sensitive to the applied criterion. However, the principle of local symmetry gives a larger branching angle, which is more consistent with experimental observations. Finally, it is shown that an increasing fracture energy with the velocity results in a decrease in the critical velocity at which branching is energetically possible.

This paper is organized as follows. In Section 2, the results concerning the general elastostatic problem of a crack of finite length with two side-branches of infinitely small lengths are presented. Although the material of this section can be found elsewhere (Smith, 1968; Amestoy and Leblond, 1992), the results are recalled here for completeness, since they are used in the subsequent analysis of the dynamic crack branching problem. In Section 3, the model problem for the determination of the dynamic stress intensity factors after branching is presented. It is shown that the formulation of such a problem for both the plane and the anti-plane loading configurations are equivalent. The similarity between these two problems allows us to propose that even under plane loading configuration, the maximum of the energy release rate immediately after

branching is attained when the branches propagate quasi-statically. In Section 4, these results are combined with Eshelby's approach for determining a crack branching criterion, and computing the critical branching quantities. In the last Section, the results are compared with experimental data, and their relevance with respect to other models of dynamic crack branching is discussed.

2. The static branching problem

Let us start by giving the general solution of the elastostatic problem depicted in Fig. 1. An infinite sheet is stretched in the presence of a crack contour consisting of a main crack of length L and two symmetric side branches of equal lengths l emerging from a common origin. The angle between the two side-branches is denoted by $2\pi\lambda$, with $0 < \lambda < 1$. In particular, the case of a main crack with two side-branches of infinitely small lengths is studied. The complex stress function method is used and the stress intensity factors are derived. In the following, the resolution of the mode III loading is given in details, while the mixed mode I–II loading is briefly presented. Detailed analysis of a similar problem can be found in (Amestoy and Leblond, 1992).

2.1. Mapping function

The mapping of the exterior of the star shape crack in the z-plane, $z = x + \mathrm{i}y$, onto the exterior of the unit circle in the ζ-plane, $\zeta = \xi + \mathrm{i}\eta$, is considered. The conformal mapping of the contour depicted in Fig. 1 is given by the function (Smith, 1968)

$$z = \omega(\zeta) = A\,\zeta^{-1}(\zeta - 1)^{2\lambda}\left[(\zeta - \mathrm{e}^{-\mathrm{i}\alpha})(\zeta - \mathrm{e}^{\mathrm{i}\alpha})\right]^{(1-\lambda)}, \tag{1}$$

where A and α are real positive constants. As can be seen from Fig. 1, The points $\zeta_k = \mathrm{e}^{\mathrm{i}\beta_k}$, $(k = 1, 2, 3)$, corresponding to the tips B_k of the star shape crack in the z-plane,

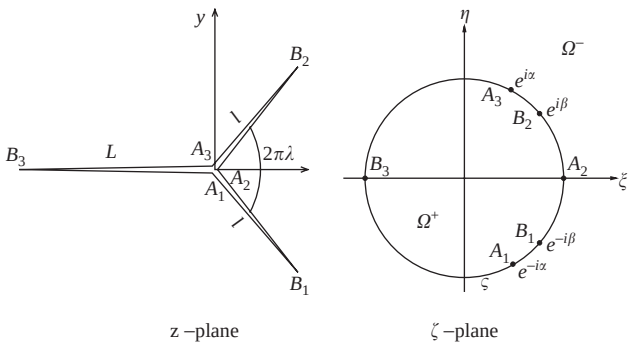

Fig. 1. Conformal mapping of a star shape crack in the z-plane onto the exterior of the unit circle in the ζ-plane. The x-axis is taken to be parallel to the main crack, and the argument of z is defined in the interval $[-\pi, \pi]$.

are the maxima of $\omega(\zeta)$. Their values are given by

$$\beta_3 = \pi; \quad \beta_2 = -\beta_1 = \beta \equiv 2\,\mathrm{Arcsin}\left(\sqrt{\lambda}\sin\frac{\alpha}{2}\right). \tag{2}$$

Then, the lengths of the cracks L and l can be expressed under the form

$$L = 4A\left(\cos\frac{\alpha}{2}\right)^{2(1-\lambda)}, \tag{3}$$

$$l = 4A\,\lambda^{\lambda}(1-\lambda)^{(1-\lambda)}\left(\sin\frac{\alpha}{2}\right)^2. \tag{4}$$

Eqs. (2)–(4) yield a unique solution of the conformal mapping parameters A, α and β as functions of l, L, and λ. In the vicinity of the tips B_k, the mapping function $z=\omega(\zeta)$ satisfies the following behavior

$$z - z_k \equiv \omega(\zeta) - \omega(\zeta_k) = \frac{1}{2}\,w''(\zeta_k)(\zeta-\zeta_k)^2, \tag{5}$$

$$\omega'(\zeta) = w''(\zeta_k)(\zeta-\zeta_k) = \sqrt{2w''(\zeta_k)(z-z_k)}. \tag{6}$$

In particular, at the point B_2 one has

$$\omega''(\zeta_2) = 4A\left(\frac{\lambda}{1-\lambda}\right)^{\lambda}\cos^2\left(\frac{\beta}{2}\right)(1+\cos^2\beta)\,\mathrm{e}^{\mathrm{i}(\lambda\pi-2\beta)}. \tag{7}$$

In the following, we will focus on the limiting case of a main crack of length L with two symmetric side branches of lengths l, with $l/L=\varepsilon\ll 1$. Consequently, to leading order in ε, Eqs. (2)–(4), (7) give

$$A = \frac{L}{4}, \tag{8}$$

$$\alpha = 2\,\lambda^{\lambda/2}(1-\lambda)^{(1-\lambda)/2}\sqrt{\varepsilon}, \tag{9}$$

$$\beta = 2\,\lambda^{(1+\lambda)/2}(1-\lambda)^{(1-\lambda)/2}\sqrt{\varepsilon}, \tag{10}$$

$$\omega''(\zeta_2) = 2L\left(\frac{\lambda}{1-\lambda}\right)^{\lambda}\mathrm{e}^{\mathrm{i}\lambda\pi}. \tag{11}$$

2.2. The mode III loading

For anti-plane strain deformation, the displacement $u_3(x,y)$ normal to the xy plane satisfies Laplace's equation

$$\Delta u_3 = 0. \tag{12}$$

A traction free boundary conditions are taken on crack surfaces, and the infinite elastic body is supposed to be loaded by an external shear stress σ_{23}^{∞}. These conditions are written

$$\vec{n}\cdot\vec{\nabla}u_3 = 0 \quad \text{on the crack surfaces,} \tag{13}$$

$$\sigma_{23} + \mathrm{i}\sigma_{13} = \sigma_{23}^{\infty} \quad \text{at infinity.} \tag{14}$$

The displacement and stress fields can be expressed by means of a complex function $\Phi(z)$, which is holomorphic outside the crack contour. In the z-plane, one has

$$u_3 = \frac{1}{2\mu}\left[\Phi(z) + \overline{\Phi(z)}\right], \tag{15}$$

$$\sigma_{13} - \mathrm{i}\sigma_{23} = \Phi'(z), \tag{16}$$

where μ is the Lamé shear coefficient and the bar indicates the complex conjugate. Note that $\overline{\Phi(z)}$ is a complex function which is holomorphic inside the crack contour. The problem can be easily solved in the ζ-plane. The boundary conditions (13), (14) read

$$\Phi(\zeta) - \overline{\Phi(\zeta)} = 0 \quad \text{as } |\zeta| \to 1^+, \tag{17}$$

$$\Phi'(\zeta) = -\mathrm{i}\sigma_{23}^{\infty} A \text{ as } \quad |\zeta| \to \infty. \tag{18}$$

The solution is readily obtained if $\Phi(\zeta)$ is given by (Smith, 1968)

$$\Phi(\zeta) = -\mathrm{i}\sigma_{23}^{\infty} A[\zeta - \zeta^{-1}]. \tag{19}$$

The stress intensity factor K_3' at the tip B_2 is defined by

$$K_3' = \lim_{z \to z_2} \sqrt{2\pi(z - z_2)}\,(\sigma_{23} + \mathrm{i}\sigma_{13})\mathrm{e}^{\mathrm{i}\lambda\pi}. \tag{20}$$

Using the behavior of $\Phi(\zeta)$ when $\zeta \to \zeta_2$, and relating it to the square root singularity of the stress field leads to:

$$K_3' = i\Phi'(\zeta_2)\sqrt{\frac{\pi \mathrm{e}^{\mathrm{i}\lambda\pi}}{w''(\zeta_2)}}. \tag{21}$$

One can easily verify that this quantity is real. For the limiting case where the two side-branches are of infinitely small lengths, it can be shown that

$$K_3' = F_{33}(\lambda) K_{03}, \tag{22}$$

where $K_{03} = \sigma_{23}^{\infty}\sqrt{\pi L/2}$ is the stress intensity factor of the main crack of length L in the absence of the side-branches. The function F_{33} is given by

$$F_{33}(\lambda) = \frac{1}{\sqrt{2}}\left[\frac{1-\lambda}{\lambda}\right]^{\lambda/2}. \tag{23}$$

The function $F_{33}(\lambda)$ as given by Eq. (23) is universal in the sense that it is independent of the applied loading. The discontinuity introduced by the vertices A_j is not intuitive, since the stress intensity factor dependence of λ is not given by a simple angular contribution. As shown in Fig. 2, the function $F_{33}(\lambda)$ displays a maximum at a branching angle corresponding to $\lambda = 0.22$.

2.3. The mixed mode I–II loading

In the following, the branching problem in plane situation is presented briefly. Effectively, the approach is analogous to the kinked crack problem which has been studied

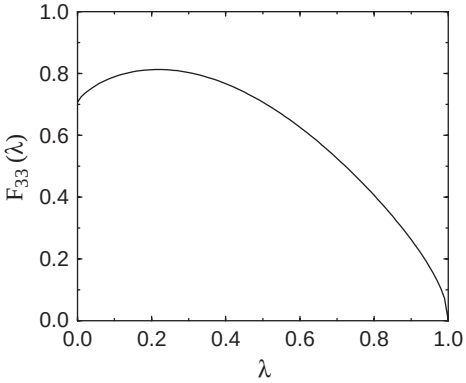

Fig. 2. Plot of the function $F_{33}(\lambda)$ as defined by Eq. (23).

previously (Amestoy and Leblond, 1992). More details of the analysis can be found in (Amestoy and Leblond, 1992) and references therein.

According to Muskhelishvili (1953), the stresses at a point $z=x+\mathrm{i}y=\omega(\zeta)$ can be expressed, in the ζ-plane, by the complex stress functions $\Phi(\zeta)$ and $\Psi(\zeta)$. For the case where traction free boundary conditions are taken on the crack surfaces and where the loading is given by external stresses σ_{11}^{∞}, σ_{22}^{∞} and σ_{12}^{∞}, the complex stress functions satisfy the following conditions

$$\Phi(\zeta)+\frac{\omega(\zeta)}{\overline{\omega'(\zeta)}}\overline{\Phi'(\zeta)}+\overline{\Psi(\zeta)}=Cte \quad \text{for } |\zeta|\to 1^{+}, \tag{24}$$

$$\Phi(\zeta)=\Gamma A \quad \text{for } |\zeta|\to\infty, \tag{25}$$

$$\Psi(\zeta)=\Gamma' A \quad \text{for } |\zeta|\to\infty, \tag{26}$$

where $\Gamma=(\sigma_{11}^{\infty}+\sigma_{22}^{\infty})/4$ and $\Gamma'=(\sigma_{22}^{\infty}-\sigma_{11}^{\infty})/2+\mathrm{i}\sigma_{12}^{\infty}$.

We focus on the asymptotic case where the two side-branches are of infinitely small lengths. Let us perform a second conformal mapping given by

$$\zeta=\exp \mathrm{i}\alpha Z, \tag{27}$$

which maps the region $|\zeta|>1$ onto the domain $\Im Z<0$ (see Fig. 3).

Following the same steps as in (Amestoy and Leblond, 1992), one finds that the problem reduces to resolving the integral equation

$$U(Z)=K_0+(1-\mathrm{e}^{-2\mathrm{i}\pi\lambda})\int_{-1}^{0} q(t)\,\frac{\overline{U(t)}}{(t-Z)^2}\,\frac{\mathrm{d}t}{4\mathrm{i}\pi} +(1-\mathrm{e}^{2\mathrm{i}\pi\lambda})\int_{0}^{1} q(t)\,\frac{\overline{U(t)}}{(t-Z)^2}\,\frac{\mathrm{d}t}{4\mathrm{i}\pi}, \tag{28}$$

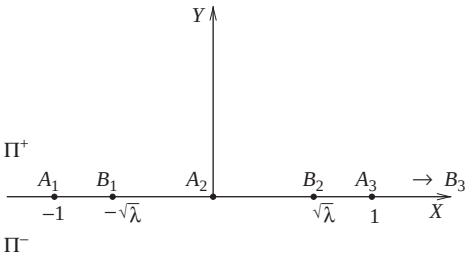

Fig. 3. The Z-plane corresponding to the conformal mapping $\zeta = \exp \mathrm{i}\alpha Z$.

where

$$U(Z) = \sqrt{\frac{8\pi}{L}}\Phi'(Z), \tag{29}$$

is a holomorphic function in the domain $\Im Z < 0$. The function $q(t)$ in Eq. (28) is given by

$$q(t) = \frac{t(t^2-1)}{(t+\sqrt{\lambda}+\mathrm{i}\varepsilon)(t-\sqrt{\lambda}+\mathrm{i}\varepsilon)}. \tag{30}$$

The term K_0 in Eq. (28) is the complex stress intensity factor of the main crack of length L in the absence of the side-branches. It is given by

$$K_0 = K_{01} - \mathrm{i}K_{02} = (\sigma_{22}^{\infty} - \mathrm{i}\sigma_{12}^{\infty})\sqrt{\frac{\pi L}{2}}. \tag{31}$$

On the other hand, it can be shown (Amestoy and Leblond, 1992) that the complex stress intensity factor K' at the crack tip B_2 is given by

$$K' = K_1' - \mathrm{i}K_2' = F_{33}(\lambda)\mathrm{e}^{-\mathrm{i}\lambda\pi}U(\sqrt{\lambda}), \tag{32}$$

which depends of the branching angle and linearly of the stress intensity factors K_{01} and K_{02}. This result is also universal in the sense that it is independent of the applied loading. Once the integral Eq. (28) is solved, the stress intensity factors K_1' and K_2' are uniquely determined. For this purpose, a useful decomposition of $U(Z)$ is given by

$$U(Z) = K_{01}U_1(Z) - \mathrm{i}K_{02}U_2(Z). \tag{33}$$

Eq. (28) is now decomposed into two independent equations

$$U_{1,2}(Z) = 1 \pm (1-\mathrm{e}^{-2\mathrm{i}\pi\lambda})\int_{-1}^{0} q(t)\,\frac{\overline{U_{1,2}(t)}}{(t-Z)^2}\,\frac{\mathrm{d}t}{4\mathrm{i}\pi}$$
$$\pm(1-\mathrm{e}^{2\mathrm{i}\pi\lambda})\int_{0}^{1} q(t)\,\frac{\overline{U_{1,2}(t)}}{(t-Z)^2}\,\frac{\mathrm{d}t}{4\mathrm{i}\pi}. \tag{34}$$

Eq. (34) can be easily computed numerically using an iterative method similar to the one used in determining the corresponding functions for the kinked crack problem. The computation of the functions $U_1(Z)$ and $U_2(Z)$ can be performed on any curve belonging to the lower half Z-plane, and that includes the points A_1, A_2 and A_3. The details of this method can be found in (Amestoy and Leblond, 1992).

Finally, the main results of this section can be summarized as follow. The stress intensity factors immediately after branching at the crack tip B_2 of the infinitely small side-branch are related to the stress intensity factors of the main crack of length L in the absence of the side-branches by the vectorial equation

$$\begin{pmatrix} K_1' \\ K_2' \\ K_3' \end{pmatrix} = \begin{pmatrix} F_{11}(\lambda) & F_{12}(\lambda) & 0 \\ F_{21}(\lambda) & F_{22}(\lambda) & 0 \\ 0 & 0 & F_{33}(\lambda) \end{pmatrix} \begin{pmatrix} K_{01} \\ K_{02} \\ K_{03} \end{pmatrix}. \tag{35}$$

The elements of the matrix F in Eq. (35) are given by

$$F_{11}(\lambda) = F_{33}(\lambda)\Re\left[e^{-i\pi\lambda}U_1(\sqrt{\lambda})\right], \tag{36}$$

$$F_{12}(\lambda) = F_{33(\lambda)}\Im\left[e^{-i\pi\lambda}U_2(\sqrt{\lambda})\right], \tag{37}$$

$$F_{21}(\lambda) = -F_{33}(\lambda)\Im\left[e^{-i\pi\lambda}U_1(\sqrt{\lambda})\right], \tag{38}$$

$$F_{22}(\lambda) = F_{33}(\lambda)\Re\left[e^{-i\pi\lambda}U_2(\sqrt{\lambda})\right] \tag{39}$$

and $F_{33}(\lambda)$ is given by Eq. (23). The remaining elements in Eq. (35) are computed once Eq. (34) are solved numerically. The corresponding results are summarized in Figs. 2 and 4.

3. The dynamic branching problem

The process of dynamic crack branching can be decomposed as follows. A semi-infinite straight crack that propagates at a speed $v(t)$ for $t < 0$ suddenly stops at $t = -\tau$, with $\tau \to 0^+$. At $t \to 0^+$, the crack branches locally with a branching angle equal to $\lambda\pi$ (see Fig. 5). For $t > 0$, the new branches propagate straightly at a velocity $v'(t)$, following the new directions $\pm\lambda\pi$. It is well established (Kostrov, 1975; Freund, 1990) that the dynamic stress intensity factors, $K_l(t)$, of the straight crack prior to branching are related to the rest stress intensity factors, $K_{0l}(t)$, of the same configuration by

$$K_l(t) = k_l(v)K_{0l}(t), \tag{40}$$

where $k_l(v)$, $l = 1, 2, 3$, are known universal functions of the instantaneous crack tip speed $v(t)$. Their explicit forms can be found in (Freund, 1990).

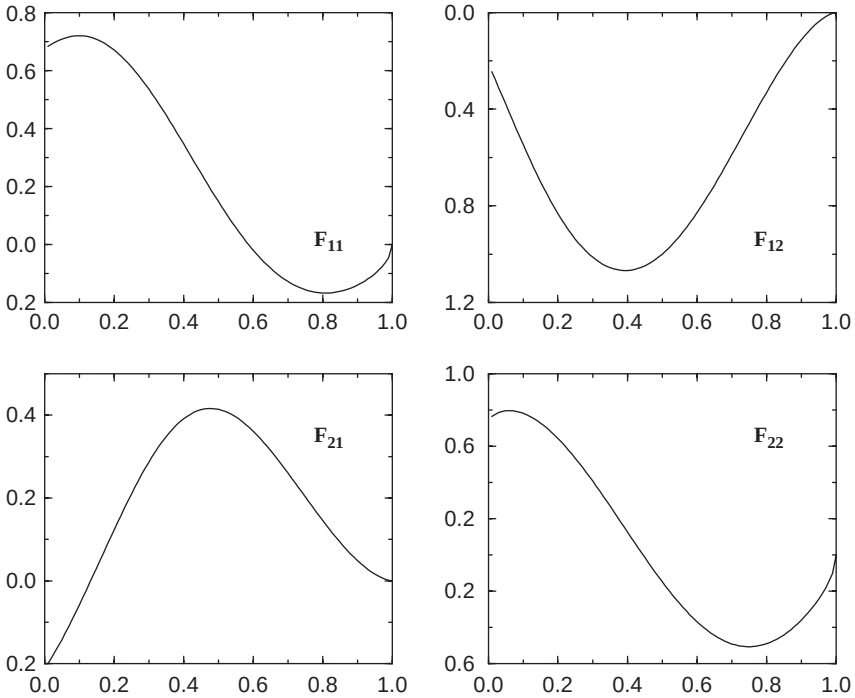

Fig. 4. Plot of the elements of the matrix $F_{lm}(\lambda)$ as defined by Eqs. (36)–(39).

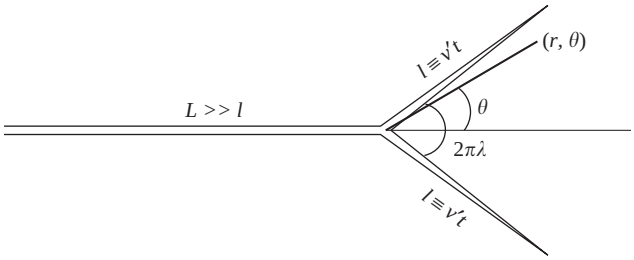

Fig. 5. Schematic representation of the dynamic branching problem.

Since there is no time scale, and consequently no length scale, against which the independent variables can be scaled, the dynamic stress intensity factors immediately after branching, K'_l for $t \to 0^+$, at each crack tip can always be written in the form of a universal function of the velocities and branching angle multiplying the rest stress intensity factors before branching, K_{0l} for $t \to 0^-$

$$K'_l = \sum_m k_l(v')H_{lm}(\lambda, v, v')K_{0m}. \tag{41}$$

As in the quasi-static case (Leblond, 1989), the matrix H is universal in the sense that it depends neither on loading configuration nor on the geometry of the body. Indeed in the limits $t \to 0^+$ and $\tau \to 0^+$ that are considered, the dynamic branching problem does not involve radiation effects, so it is always equivalent to a crack propagating in an unbounded body. Moreover, H should approach the elastostatic solution for a vanishingly small velocity of the side-branches

$$\lim_{v' \to 0} H_{lm}(\lambda, v, v') = F_{lm}(\lambda). \tag{42}$$

The present dynamic branching problem consists in determining the behavior of the matrix H as a function of the branching angle and of the instantaneous velocities immediately before and immediately after branching. In the following, the results of the anti-plane case are recalled (Adda-Bedia and Arias, 2003; Adda-Bedia, 2004), and the model problem for the determination of the plane dynamic stress intensity factors immediately after branching is presented.

3.1. The mode III loading

Under anti-plane loading conditions, it is known that when the initial crack stops, a static stress distribution is restored behind a wave front that propagates from the crack tip at the shear wave speed (Eshelby, 1969; Freund, 1990). Thus for $t > 0$, the propagation of the branches occurs within a stationary stress field induced by the arrest of the original single crack. Moreover, in the limit $t \to 0^+$, the lengths of the branched parts of the crack are vanishingly small, so that the breaking process after branching occurs in the region determined by the square root singular stress intensity factor field of the semi-infinite straight crack. Therefore, the dynamic branching problem consists of two symmetric branches reminiscent from a preexisting stationary straight crack, that start to propagate at time $t = 0$, in the directions $\pm\lambda\pi$, by negating a time-independent traction distribution on the newly broken surfaces given by (Williams, 1952)

$$\sigma_{23}^{(s)}(r < v't, \pm\lambda\pi) = \frac{K_{03}}{\sqrt{2\pi r}} \cos\frac{\lambda\pi}{2}, \tag{43}$$

where K_{03} is the rest stress intensity factor of the crack tip prior to branching. A direct consequence of Eq. (43) is that the matrix element H_{33} must be independent of the velocity prior to branching.

$$H_{33}(\lambda, v, v') \equiv H_{33}(\lambda, v'/c_s). \tag{44}$$

Using these arguments, a method for determining the elastodynamic stress fields associated with the propagation of branched cracks was developed in (Adda-Bedia, 2004). Particularly, it was shown that the corresponding model problem admits a self-similar solution, which is a convolution integral between a known kernel and a harmonic function that satisfies a simple integral equation. Once the integral equation is solved, the stress intensity factor immediately after branching is computed *a posteriori* using an additional condition. The function H_{33} can then be computed *exactly* as a function of the branching angle λ and of the instantaneous velocity v'.

3.2. The mixed mode I–II loading

Under plane loading situations, when the initial crack stops, the static stress distribution is restored in the crack plane only (Freund, 1990); ahead of the crack tip, this happens behind a wave front that propagates at the shear wave speed, c_s, and behind the crack tip, behind a wave front that propagates at the Rayleigh wave speed, c_R. These two properties are sufficient to determine the dynamics of a single crack moving straightly (Freund, 1990). However, for a dynamic crack of arbitrary path, one has to specify the whole angular distribution of the stress field in the vicinity of the crack tip induced by the crack arrest, which is given by (Kostrov, 1975; Madariaga, 1977)

$$\sigma_{ij}^{(d)}(r,\theta,t) = \frac{K_{01}(t+\tau)}{\sqrt{2\pi r}}\, f_{ij}^{(1)}(\chi,\theta) + \frac{K_{02}(t+\tau)}{\sqrt{2\pi r}}\, f_{ij}^{(2)}(\chi,\theta), \tag{45}$$

where c is a characteristic wave speed of the material, K_{01} and K_{02} are the rest stress intensity factors of the crack tip prior to branching, and

$$\chi \equiv \frac{r}{c(t+\tau)}. \tag{46}$$

Here, the time delay τ is present because of our decomposition of the branching process.

Therefore, contrary to the anti-plane case, the present branching problem should be expressed as follows. Two symmetric branches reminiscent from a preexisting stationary straight crack, start to propagate at time $t=0^+$, in the directions $\pm\lambda\pi$, with a velocity v', by negating a traction distribution on the newly created surfaces, $\sigma_{ij}^{(d)}$ $(r < v't, \pm\lambda\pi, t)$, given by Eq. (45). Due to the presence of both dilatational and shear elastic waves, there is no sharp limit between the dynamic and the static distributions of the stress fields in the neighborhood of the crack tip. Indeed, the stress distributions at any point off the crack plane relax continuously and reach the static distributions for $\chi \to 0$ only (Kostrov, 1975; Madariaga, 1977)

$$\lim_{\chi\to 0} f_{ij}^{(l)}(\chi,\theta) = \Sigma_{ij}^{(l)}(\theta), \tag{47}$$

where $\Sigma_{ij}^{(l)}$ are the well-known angular variations of the static square root singular stress intensity factor field (Williams, 1952).

Thus in general, the propagation of the branches does not occur within stationary stress fields. Moreover, the functions $f_{ij}^{(l)}$ depend explicitly on the crack tip velocity prior to the crack arrest (Madariaga, 1977). Therefore, contrary to the mode III case, the elements of the matrix H_{lm} corresponding to the inplane configuration can depend explicitly on the velocity before branching. However, the determination of the stress fields immediately after branching makes the problem simpler. Since the single straight crack stops at $t=-\tau$, with $\tau \to 0^+$, and the branches start to propagate at $t \to 0^+$, one always has

$$\chi \equiv \frac{r}{c(t+\tau)} < \frac{v't}{c(t+\tau)} \to 0. \tag{48}$$

We emphasize on the importance of the order in which the limits must be taken. The decomposition of the crack branching process as described above imposes that the limit $t \to 0^+$ must be taken before the limit $\tau \to 0^+$. Therefore, the stress intensity factor

field immediately after branching is determined by solving a branching problem where the traction distribution that has to be negated during the propagation of the branches is given by the static square root singular stress intensity factor field of the initial straight crack

$$\sigma_{ij}^{(s)}(r < v't, \pm\lambda\pi, t) = \frac{K_{01}}{\sqrt{2\pi r}}\Sigma_{ij}^{(1)}(\pm\lambda\pi) + \frac{K_{02}}{\sqrt{2\pi r}}\Sigma_{ij}^{(2)}(\pm\lambda\pi), \tag{49}$$

Therefore, the dependence of the velocity of the single crack tip before branching is suppressed from the stress distribution that has to be negated during the propagation of the branches. Consequently, the matrix elements H_{lm} related to plane loading situations should be also independent of the velocity prior to branching.

$$H_{lm}(\lambda, v, v') \equiv H_{lm}(\lambda, v'/c). \tag{50}$$

It is important to notice that the stress intensity factors immediately after branching involve the history of crack propagation before branching only through the rest stress intensity factors. More precisely, they do not have any explicit dependence of the velocity of the single crack tip. This important result is mainly due to the absence of intrinsic time or length scales in linear elasticity theory. Similarly to what happens in the anti-plane case, the property (49) implies that the resulting elastic fields should exhibit self-similar properties. However, the in-plane configuration is characterized by two displacement potentials that satisfy wave equations with two different wave speeds (Broberg, 1999; Freund, 1990). Thus, self-similar solutions of the displacement potentials are necessarily given in terms of two different self-similar "coordinates"; $(c_s t/r, \theta)$ and $(c_d t/r, \theta)$, where c_d (c_s) is the dilatational (shear) wave speed. The coupling between the dilatational and shear elastic waves makes the complete resolution of the resulting problem unapproachable. However, the similarity between the mode III and the in-plane problems suggests that the main features of the mode III results should be preserved.

4. Dynamic branching instability

A growth criterion for a branched crack must be based on the equality between the energy flux into each propagating tip and the surface energy which is added as a result of this propagation (Griffith, 1920). The dynamic energy release rate is defined as the rate of mechanical energy flow out of the body and into the crack tip per unit crack advance. It is well established that the energy release rate G for a single straight crack is given by (Kostrov, 1975; Freund, 1990)

$$G = \frac{1}{2\mu}\sum_{l=1}^{3} A_l(v)K_l^2 = \frac{1}{2\mu}\sum_{l=1}^{3} g_l(v)K_{0l}^2, \tag{51}$$

where μ is the Lamé shear coefficient, and

$$g_l(v) = A_l(v)k_l^2(v). \tag{52}$$

The functions $A_l(v)$ and $g_l(v)$ do not depend on the details of the applied loading or on the configuration of the body being analyzed. They only depend on the local

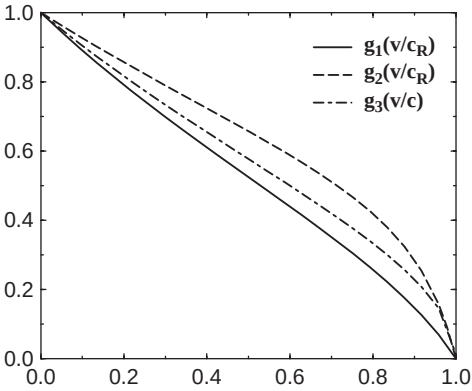

Fig. 6. Plot of the universal functions $g_1(v/c_R)$, $g_2(v/c_R)$ and $g_3(v/c_s)$ for $(c_d/c_s)^2 = 3$. Here, c_d (resp. c_s) denotes the dilatational (resp. shear) wave speed of the material.

instantaneous speed of the crack tip and on the properties of the material only. For completeness, the functions $g_I(v)$ are reproduced in Fig. 6.

The dynamic energy release rate is a quantity associated to a single moving crack tip. Thus, after branching one has to determine it for each crack tip. Due to the symmetry of the branching configuration, the energy release rate immediately after branching G' for each crack tip is given by

$$G' = \frac{1}{2\mu}\sum_{I=1}^{3} A_I(v') K'^2_I. \tag{53}$$

When the initial single crack is propagating under a mode III loading, Eq. (53) reduces to

$$G'_3 = \frac{1}{2\mu}\, g_3(v') H^2_{33}(\lambda, v'/c_s) K^2_{03}, \tag{54}$$

where K_{03} is the rest stress intensity factor immediately before branching. In (Adda-Bedia, 2004), it has been shown that for a constant branching angle, G'_3 is a decreasing function of v'. Therefore, the energy release rate immediately after branching is maximized when the branches start to propagate quasi-statically ($v' \to 0$), that is when $G'_3 \equiv G'^{(s)}_3$. Equivalently, if the loading configuration before branching is of mode I type, the energy release rate immediately after branching G'_1 at each crack tip is given by

$$G'_1 = \frac{1}{2\mu}\left[g_1(v') H^2_{11}(\lambda, v'/c_s) + g_2(v') H^2_{21}(\lambda, v'/c_s)\right] K^2_{01}, \tag{55}$$

where K_{01} is the rest stress intensity factor immediately before branching. At the present stage, the exact computation of the energy release rate immediately after branching under in-plane configurations is not possible. Nevertheless, the exact resolution of the mode III problem does give indications about the general behavior of G'_1. Indeed, in many physical aspects of crack propagation, the results corresponding to mode III and

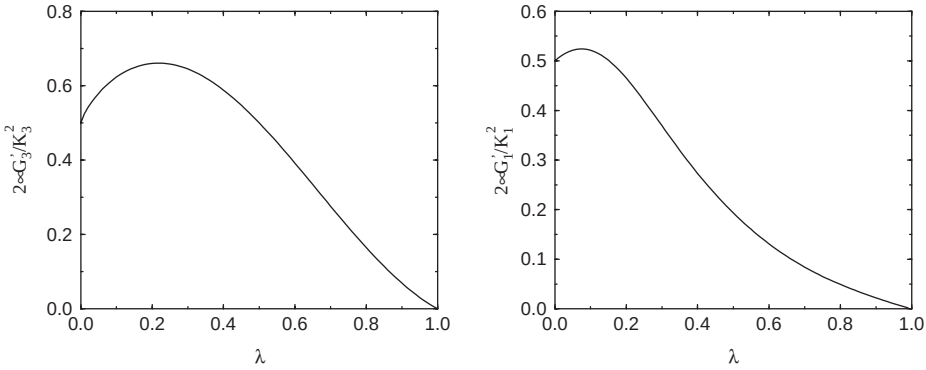

Fig. 7. Plot of the maximum energy release rate immediately after branching as a function of the branching angle, for the cases of a mode III loading (left) and a mode I loading (right).

to in-plane configurations are qualitatively similar (Broberg, 1999; Freund, 1990). As for the anti-plane case, the in-plane elastic fields immediately after branching exhibit self-similar properties, and the corresponding stress intensity factors do not depend explicitly of the velocity of the single crack tip before branching. These similar properties allow to predict the general behavior of the energy release rate immediately after branching.

The results of (Adda-Bedia, 2004) show that $H_{33}(\lambda, v'/c_s)$ depends only weakly on v'. Indeed, the ratio $H_{33}(\lambda, v'/c)/F_{33}(\lambda)$ is very close to unity (up to $\pm 5\%$) for all values of λ and v'/c_s. The similarity between the anti-plane and the in-plane branching problem suggests that this behavior should be maintained for all the matrix elements $H_{lm}(\lambda, v'/c)$. Therefore, one expects that the energy release rate immediately after branching for in-plane configurations is also maximized when the branches start to propagate quasi-statically ($v' \to 0$), that is when $G_1' \equiv G_1'^{(s)}$. Let us emphasize that this property results from arguments deduced from the analogy with the anti-plane results. Even if this property does not hold exactly for in-plane configurations, the analogy with the anti-plane case suggests that it is a good approximation. Nevertheless, a complete resolution of the in-plane dynamic branching problem would be necessary to check this hypothesis. Fig. 7 displays the plots of $G_3'^{(s)}$ and $G_1'^{(s)}$ as functions of the branching angle. It is shown that their behavior are qualitatively equivalent. They are both equal to $1/2$ for "zero" branching angle and they both display a maximum at a given branching angle.

According to the generalized Griffith criterion (Griffith, 1920), the crack must grow in such a way that the energy release rate is always equal to the dynamic fracture energy of the material, $\Gamma(v)$, which is assumed to be a property of the material and whose value may depend on the instantaneous crack tip speed (Boudet et al., 1996; Sharon and Fineberg, 1999). This growth criterion, $G \equiv \Gamma(v)$, should be applied for the crack tips before and after branching. This insures that each crack tip is always propagating according to the Griffith criterion. Therefore, the growth criterion introduces an intrinsic

relation between the energy release rates immediately before and immediately after branching, which reads

$$G' = \frac{\Gamma(v')}{\Gamma(v)}\, G. \tag{56}$$

Eq. (56) is a necessary condition for the existence of a branching configuration. Otherwise, the single crack tip propagation should be maintained. This equation, however, is not a sufficient condition for determining the branching threshold parameters, which must be deduced from some other criteria. For instance, the maximum energy release rate criterion (Erdogan and Sih, 1963) or the principle of local symmetry (Gol'dstein and Salganik, 1974). These two criteria have been applied essentially to problems related to the selection of single quasi-static crack paths, and give almost similar numerical predictions. However, it has been shown that the principle of local symmetry is more coherent and it is now widely admitted as the second additional equation of motion (Leblond, 1989; Adda-Bedia et al., 1999). In the following, these two criteria will be used to predict the branching instability and will be compared with the experimental results.

4.1. The maximum energy release rate (MERR) criterion

Eshelby (1970) posed the question of how large must be the single crack velocity v, so that by decelerating, there is enough energy available to form two cracks propagating at a velocity v'. This approach can be interpreted as being equivalent to the maximum energy release rate criterion. Since the energy release rate after branching is always largest when $v' \to 0$, the maximum energy release rate after branching depends of the branching angle only.

Let us start by the case of constant fracture energy and focus on the in-plane crack propagation. Using Eq. (56), one deduces that the critical velocity before branching must be a solution of

$$g_1(v) = F_{11}^2(\lambda) + F_{21}^2(\lambda). \tag{57}$$

Fig. 6 shows that $g_1(v)$ is a decreasing function of the velocity that satisfies $g_1(0)=1$, and $g_1(c_R)=0$. On the other hand, the right-hand side of Eq. (57) displays a maximum, whose value is less than unity (see Fig. 7). Therefore, this equation is not always satisfied, and branched solutions exist when the velocity v exceeds a critical velocity v_c only. This threshold value is given by the least velocity v for which Eq. (57) admits a solution. It corresponds to a branched solution with a non-vanishing branching angle, $\lambda_c = 0.07$, given by the maximum of $F_{11}^2(\lambda)+F_{21}^2(\lambda)$, and a corresponding critical speed, $v_c \approx 0.5 c_R$, given by Eq. (57).

4.2. The principle of local symmetry (PLS)

While the MERR criterion states that the crack should follow a direction of maximum energy release rate, the principle of local symmetry states that the path taken by a crack in a brittle homogeneous isotropic material is the one for which the local stress field

Table 1
Branching thresholds v_c and λ_c for different branching criteria and loading modes. For the inplane case, the thresholds are given using a Poisson ratio such that $(c_d/c_s)^2 = 3$

	MERR, mode III	MERR, mode I	PLS, mode I
v_c	0.392 c_s	0.503 c_R	0.518 c_R
λ_c	0.22	0.07	0.13

at the tip is of mode I type (Gol'dstein and Salganik, 1974). It is not obvious that the crack propagation still satisfies this criterion in the dynamic case. However, there is an argument in favor of this scenario (Adda-Bedia et al., 1999). The dynamic energy release rate can be seen as the component, F_1, of the configurational force along the direction of crack motion. The Griffith energy criterion can thus be reinterpreted as a material force balance between F_1 and a resistance force to crack advance per unit length of the crack front: $F_1 \equiv \Gamma$. However, this equation of motion is not sufficient to determine the trajectory of a crack if it is allowed to deviate from straight propagation. If one assumes that configurational forces balance holds at the crack tip, one should also impose that the component of the material force perpendicular to the direction of crack propagation must vanish (Adda-Bedia et al., 1999). Since this quantity is proportional to K_2, it results that the crack propagation occurs in such a way as to keep a purely opening mode at its tip.

In the case of PLS, at any stage of crack propagation two equations of motion must be fulfilled: the Griffith energy criterion and the pure opening condition at the crack tip. When a main crack subjected to a mode I loading branches into two symmetric cracks, these conditions are satisfied by the single crack tip prior to branching as long as the crack tip follows a straight path. On the other hand, immediately after branching, these two conditions must be written as

$$g_1(v) = F_{11}^2(\lambda), \tag{58}$$

$$F_{21}(\lambda) = 0. \tag{59}$$

Now, the branching angle, λ_c, is selected in a different way from the MERR criterion, while the arguments for determining the critical velocity, v_c, are the same. Thus, the result of application of these equations gives also a selected branching angle and a critical speed for branching. From Table 1, it is seen that the critical branching velocity $v_c \approx 0.52 c_R$ does not differ too much from the one deduced by using MERR criterion, while the critical branching angle is twice larger, $\lambda_c = 0.13$. Note that this value is approximately equal to the branching angle $\lambda_c = 0.15$ calculated by using an analysis of a branched crack based on the body force method combined with a perturbation procedure (Isida and Noguchi, 1992).

4.3. Effect of velocity dependent fracture energy

Eq. (56) obviously shows that a velocity dependent fracture energy affects the results of the latter calculations. As the two branching criteria are based to some level on

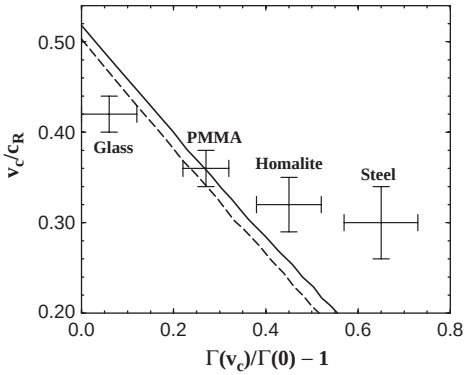

Fig. 8. Plot of the critical branching velocity for the case of velocity dependent fracture energy and for $(c_d/c_s)^2 = 3$. The solid line corresponds to the values deduced from PLS and the dashed line to those deduced from the MERR criterion. The experimental values reported are estimates taken from (Sharon and Fineberg, 1999) for Glass and PMMA, (Dally, 1979) for Homalite 100 and (Congleton, 1973; Anthony et al., 1970) for "Pitho" tool steel.

energy balance, their results should be modified by the behavior of $\Gamma(v)$. When taking into account this new degree of freedom, Eq. (57), related to MERR criterion, becomes

$$\frac{\Gamma(0)}{\Gamma(v)}\, g_1(v) = F_{11}^2(\lambda) + F_{21}^2(\lambda) \tag{60}$$

and in the case of PLS, Eq. (58) becomes

$$\frac{\Gamma(0)}{\Gamma(v)}\, g_1(v) = F_{11}^2(\lambda), \tag{61}$$

while Eq. (59) is not modified. In general, $\Gamma(v)$ is an increasing function of the velocity (Boudet et al., 1996; Sharon and Fineberg, 1999). Therefore, the left-hand side of Eqs. (60), (61) decreases faster than in the constant fracture energy case, and the energy balance can thus be achieved at lower velocity, while the critical branching angles remain the same. Although $\Gamma(v)$ can be a nonlinearly dependent function of the crack tip speed, it is only the amount of $\Gamma(v_c)/\Gamma(0)$ which is of importance in determining the critical crack tip velocity v_c. In Fig. 8, this quantity is plotted for different values of $\Gamma(v_c)/\Gamma(0)$, when either MERR criterion or PLS is applied.

5. Discussion

Under tensile mode loading, it is shown that the formulation of the problem for determining the dynamic stress intensity factors immediately after branching is identical to the anti-plane case. This analogy allows us to formulate the hypothesis that under plane loading configurations, the jump in the energy release rate due to branching is also maximized when the branches start to propagate quasi-statically. Therefore, the branching of a single propagating crack under mode I loading is found to be energetically possible when its speed exceeds a threshold value. The critical velocity v_c is only

weakly dependent on the Poisson ratio of the material, and is only slightly modified by changing the crack propagation criterion from the maximum energy release rate criterion to the principle of local symmetry (see Table 1 and Fig. 8). Still, the branching angle in the case of PLS is twice as large as the one that results from the application of MERR criterion; 23.4° instead of 12.6°. Finally, for a velocity dependent fracture energy, the critical velocity for branching v_c decreases with increasing $\Gamma(v_c)/\Gamma(0)$. The present work establishes the necessary conditions at which branching is energetically possible. It does not address the stability of the single straight propagating crack with respect to a branched configuration. In either experiments or numerical simulations, the selection mechanism might be due to the presence of noise which allows the system to visit all possible configurations.

Fig. 8 displays a comparison with estimates of critical speeds for branching taken from existing experimental data. It is shown that the predicted decrease of v_c with increasing $\Gamma(v_c)/\Gamma(0)$ is found in experiments as well. The present energy balance approach allows to obtain this result, which cannot be done in calculations based on analysis of the stress field around a single crack tip. Fig. 8 shows that except for the case of PMMA, for which there is a good agreement between the measured (Sharon and Fineberg, 1999) and the calculated critical velocity, the experimental data show a weaker dependence of v_c on $\Gamma(v_c)/\Gamma(0)$. However, the critical velocities for branching and the velocity dependence of the fracture energy for both Homalite and Steel should be taken as very rough estimates (Congleton, 1973; Anthony et al., 1970; Dally, 1979). More precise experiments on different materials are needed in order to establish the behavior of the critical speed for branching with the fracture energy dependence of the velocity. On the other hand, the critical velocity for branching is larger by 24% than the measured value for glass, a material which is commonly assumed to have a nearly constant fracture energy (Sharon and Fineberg, 1999). However, the calculated critical speed for branching, $v_c = 0.52c_R$, agrees with the one deduced from numerical simulations using a phase field model of brittle fracture under in-plane loading (Henry and Levine, 2004). In order to fit the experimental critical velocity of $0.42c_R$, a variation of fracture energy with velocity of approximately 15% is needed (see Fig. 8), which is slightly larger than the error bars of the experimental results reported in (Sharon and Fineberg, 1999).

Let us emphasize that the present work is based on exact results of the anti-plane branching problem (Adda-Bedia, 2004). Moreover, it is proven that similarly to the anti-plane case, the in-plane elastic fields exhibit self-similar properties immediately after branching, and the corresponding stress intensity factors do not explicitly depend on the velocity of the single crack tip before branching. These similar properties allow for the assumption that the main results of the mode III case should hold for in-plane configurations. Therefore, one expects that the energy release rate immediately after branching for in-plane configurations is also maximized when the branches start to propagate quasi-statically. Even if this property might not hold exactly for in-plane configurations, the analogy with the anti-plane case suggests that it must be a good approximation. One may wonder if the zero velocity immediately after branching is physically relevant, since it seems in contradiction with both experimental observations and numerical simulations. A possible explanation of this discrepancy is that the

branches start their propagation at vanishingly small speeds, but accelerate rapidly to velocities of the same order of the principal crack speed. This scenario is consistent with the results of single crack propagation in the framework of linear elastic fracture mechanics. Nevertheless, real materials are not ideally brittle and in numerical simulations one always introduces intrinsic small length scales (or time scales), which may explain the observed smooth variation of the crack speeds before and after branching. The velocity jump predicted using linear elastic fracture mechanics may be seen as an asymptotic result which is exactly valid for ideally brittle materials.

Fig. 7 shows that under mode I loading conditions, the angular variation of the energy release rate immediately after branching has a shallow maximum in the region $0 \leqslant \lambda \leqslant 0.2$. The flatness of G' at low branching angles explains the weak variation of v_c with the type of criterion applied, but is an indication in favor of the PLS versus the MERR criterion. Effectively, If the MERR criterion were the relevant one, there would not be a clear selection of the branching angle and one would expect branching for a wide range of angles. This contradicts experimental observations (Sharon et al., 1995), which show a clear selection of the branching angle. On the other hand, $F_{21}(\lambda)$ is steep around its zero value and thus, the PLS gives a well-defined selected branching angle which is equal to 23.4°, independently of the Poisson ratio of the material. Sharon et al. (1995) reported that the micro-branches which appear immediately after the onset of the branching instability are not straight. Instead, the "branching angle" increases as one approaches the branching point. Measuring the tangent to the profile of the branch at a distance of 5 μm from the branching point, the authors reported branching angles of 30° for glass and PMMA. These angles are of the same order of magnitude as the predictions of the present model based on PLS, but nearly three times larger than the predictions when using MERR. Therefore, these observations suggest that the relevant criterion for branching must be the PLS one.

Finally, previous attempts to predict the critical velocity for branching in the framework of linear elasticity were focused on the properties of the stress fields around the tip of a single fast crack (Yoffe, 1951; Freund, 1990; Adda-Bedia et al., 1996). These works indicated that above a critical velocity, a component of the singular stress field, which was regarded as the relevant one for path selection, attains a maximum off the original direction of propagation. It was suggested that in these conditions, the single straight crack solution becomes unstable. Still, none of these models dealt with the resultant state of the system, that of two branches. One must verify that the new branched state is energetically possible. The present work, which is based on Eshelby's approach, targets these points by applying growth criteria to the branched state. More recent works challenge the dynamic branching problem, using numerical simulations and calculations on the molecular scale (Abraham et al., 1994; Marder and Gross, 1995). One might argue that since the first stages of the branching process occur within the process zone, branching criteria based on continuum models are meaningless. It may be that the branching criterion must be based on processes at the molecular scale. Indeed, the present model does not target the question of when a tip of a crack will bifurcate, it determines the conditions which are necessary for the propagation of two branches. Calculations at molecular scales may show that even at lower velocities, the tip is unstable and the material tends to be opened off the original

direction. However, these flows may not be able to grow to the continuum scale. Instead, they might affect the fracture energy of the *single crack* and its fracture surface topology. As experimental data show (Sharon et al., 1995; Sharon and Fineberg, 1996), the change in the dynamics of the crack occurs simultaneously with the appearance of micro-branches of 10–100 μm length. This is certainly a continuum scale. Thus, deviations from straight crack which occur before the appearance of "continuum scale branches" do not drastically change the crack dynamics and can be included within the process zone.

Acknowledgements

I wish to thank R. Arias and J.R. Rice for enlightening discussions. I also thank E. Sharon for his comments on many experimental facts which are included in the discussion Section. Laboratoire de Physique Statistique de l'Ecole Normale Supérieure is associated with CNRS (UMR 8550) and with Universities Paris VI and Paris VII.

References

Abraham, F.F., Brodbeck, D., Rafey, R.A., Rudge, W.E., 1994. Instability dynamics of fracture, a computer simulation investigation. Phys. Rev. Lett. 73, 272–275.

Adda-Bedia, M., 2004. Brittle fracture dynamics with arbitrary paths—II. Dynamic crack branching under general antiplane loading. J. Mech. Phys. Solids 52, 1407–1420.

Adda-Bedia, M., Arias, R., 2003. Brittle fracture dynamics with arbitrary paths—I. Dynamic crack kinking under general antiplane loading. J. Mech. Phys. Solids 51, 1287–1304.

Adda-Bedia, M., Ben Amar, M., Pomeau, Y., 1996. Morphological instabilities of dynamic fracture in brittle solids. Phys. Rev. E 54, 5774–5779.

Adda-Bedia, M., Arias, R., Ben Amar, M., Lund, F., 1999. Generalized Griffith criterion for dynamic fracture and the stability of crack motion at high velocities. Phys. Rev. E 60, 2366–2376.

Amestoy, M., Leblond, J.B., 1992. Crack paths in plane situations–II. Detailed form of the expansion of the stress intensity factors. Int. J. Solids Struct. 29, 465–501.

Anthony, S.R., Chubb, J.P., Congleton, J., 1970. The crack-branching velocity. Philos. Mag. 22, 1201–1216.

Boudet, J.F., Ciliberto, S., 2000. Interaction of sound with fast crack propagation: an equation of motion for the crack tip. Physica D 142, 317–345.

Boudet, J.F., Ciliberto, S., Steinberg, V., 1996. Dynamics of crack propagation in brittle materials. J. Phys. II France 6, 1493–1516.

Broberg, K.B., 1999. Cracks and Fracture. Academic Press, London.

Congleton, J., 1973. Practical applications of crack-branching measurements, Proceedings of the International Conference on Dynamic Crack Propagation, Noordhoff International Publishing, Leiden, pp. 427–438.

Dally, J.W., 1979. Dynamic photoelastic studies of fracture. Exp. Mech. 19, 349–361.

Erdogan, G., Sih, G.C., 1963. On the crack extension in plates under plane loading and transverse shear. J. Basic Eng. 85, 519–527.

Eshelby, J.D., 1969. The elastic field of a crack extending nonuniformly under general anti-plane loading. J. Mech. Phys. Solids 17, 177–199.

Eshelby, J.D., 1970. Energy relations and the energy-momentum tensor in continuum mechanics. In: Kanninen, M.F., Adler, W.F., Rosenfield, A.R., Jaffee, R.I. (Eds.), Inelastic Behaviour of Solids. McGraw-Hill, New York, pp. 77–115.

Fineberg, J., Gross, S.P., Marder, M., Swinney, H.L., 1992. Instability in the propagation of fast cracks. Phys. Rev. B 45, 5146–5154.

Freund, L.B., 1990. Dynamic Fracture Mechanics. Cambridge University Press, New York.

Gol'dstein, R.V., Salganik, R.L., 1974. Brittle fracture of solids with arbitrary cracks. Int. J. Fract. 10, 507–523.

Griffith, A.A., 1920. The phenomenon of rupture and flow in solids. Philos. Trans. R. Soc. London A 221, 163–198.

Gross, S.P., Fineberg, J., Marder, M., McCormick, W.D., Swinney, H.L., 1993. Acoustic emission in dynamic fracture. Phys. Rev. Lett. 71, 3162–3165.

Henry, H., Levine, H., 2004. Dynamic instabilities of fracture under biaxial strain using a phase field model, cond-mat/0402563.

Isida, M., Noguchi, H., 1992. Stress intensity factors at tips of branched cracks under various loadings. Int. J. Fract. 54, 293–316.

Kostrov, B.V., 1975. On the crack propagation with variable velocity. Int. J. Fract. 11, 47–56.

Leblond, J.B., 1989. Crack paths in plane situations—I. General form of the expansion of the stress intensity factors. Int. J. Solids Struct. 25, 1311–1325.

Lobkovsky, A.E., Karma, A., 2004. Unsteady Crack Motion and Branching in a Phase-Field Model of Brittle Fracture. Phys. Rev. Lett. 92, 245510.

Madariaga, R., 1977. High-frequency radiation from crack (stress drop) models of earthquake faulting. Geophys. J. R. Atron. Soc. 51, 625–651.

Marder, M., Gross, S.P., 1995. Origin of crack tip instabilities. J. Mech. Phys. Solids 43, 1–48.

Muskhelishvili, N.I., 1953. Some basic problems of the mathematical theory of elasticity. Noordhoff, Groningen.

Ravi-Chandar, K., Knauss, W.G., 1984. An experimental investigation into dynamic fracture—III. On steady-state crack propagation and crack branching. Int. J. Fract. 26, 141–154.

Rice, J.R., Ben-Zion, Y., Kim, K.S., 1994. Three–dimensional perturbation solution for a dynamic planar crack moving unsteadily in a model elastic solid. J. Mech. Phys. Solids 42, 813–843.

Sharon, E., Fineberg, J., 1996. Microbranching instability and the dynamic fracture of brittle materials. Phys. Rev. B 54, 7128–7139.

Sharon, E., Fineberg, J., 1999. Confirming the continuum theory of dynamic brittle fracture for fast cracks. Nature 397, 333–335.

Sharon, E., Gross, S.P., Fineberg, J., 1995. Local branching as a mechanism in dynamic fracture. Phys. Rev. Lett. 74, 5096–5099.

Smith, E., 1968. Crack bifurcation in brittle solids. J. Mech. Phys. Solids 16, 329–336.

Williams, M.L., 1952. Stress singularities resulting from various boundary conditions in angular corners of plates in extension. J. Appl. Mech. 19, 526–528.

Xu, X.P., Needleman, A., 1994. Numerical simulations of fast crack growth in brittle solids. J. Mech. Phys. Solids 42, 1397–1434.

Yoffe, E.H., 1951. The moving Griffith crack. Philos. Mag. 42, 739–750.